Simulation and visualization of spraying droplets behavior and deposition within virtual rice canopy

Weilong Ding[1*], Fenglong Zhu[1], Mengjie Jin[1], Lifeng Xu[1], Yuping Zhang[2*]

(1. *College of Computer Science & Technology, Zhejiang University of Technology, Hangzhou 310023, China*;
2. *State Key Laboratory of Rice Biology, China National Rice Research Institute, Hangzhou 310006, China*)

Abstract: Models for accurately simulating pesticide droplet deposition and transmission mechanism in rice canopies can provide an effective and economic tool to optimize methods for spraying pesticides, adjuvant formulation, and spray parameters. However, the current studies on the modeling of spray droplet deposition within rice plants are still very limited. Aiming at this problem, a method to model and visualize spray transmission and deposition within the canopy of rice plants was proposed. Firstly, a particle system was used to simulate the spraying scene of droplets. Then an improved method to determine the behavior of rebound and shatter of the droplets in the virtual scene was proposed. The deposition of spraying droplets on a leaf was calculated according to the inclination angles of the leaf, the characteristics of the leaf surface, and the physical and spatial characteristics of the droplets. The experiment shows that the method can simulate the behavior of the spraying droplets within a virtual scene of a rice plant, which may provide a reference for the study of spray deposition in the canopy of the crop.
Keywords: virtual rice plant, droplet deposition, behavior simulation, spray scene

Citation: Ding W L, Zhu F L, Jin M J, Xu L F, Zhang Y P. Simulation and visualization of spraying droplets behavior and deposition within virtual rice canopy. Int J Agric & Biol Eng, 2022; 15(5): 19–27.

1　Introduction

By combining graphics and physical methods, the structure of the spray field is created, and various interaction phenomena between droplets and leaves can be observed, which can guide the study of droplet and leaf behaviors, analyze the deposition of droplets on leaves, and reduce the time and labor needed for performing field experiments.

At present, studies on the visualization of plant spray scenes at home and abroad mainly focus on the following aspects: 1) modeling of droplets and spray based on computer graphics methods, which focuses on realistically rendering droplets and spray; 2) modeling the interactions between plants and environmental factors, which focuses on the study of various phenomena between them based on physical laws, such as the deposition, rebound, and shatter of the droplets and plant growth and deformation under the influence of environmental factors; and 3) research related to plant sprays in agriculture, which focuses on the quantitative study of deposition under the effects of fog characteristics, plant topology, and leaf surface characteristics, such as studying the effects of spray equipment, spray methods[1,2],

chemical components[3,4], size and velocity of the droplets in the spray field[5], plant morphology[5], and rice leaf characteristics[6] on the amounts of deposited droplets on crops. These studies have obtained a considerable amount of effective spray parameter data, which can guide the optimization of spray parameters. However, these methods are mainly based on experiments performed in farms and spray chambers. The experiment is time- and labor-consuming and easily affected by the external environment.

The physical properties of the interactions between environmental factors and plants play an active role in studying the interaction mechanism and predicting the growth of plants under the influence of external environments. Studies on the interaction between droplets and solid surfaces have been performed[7], but research on the interaction between droplets and crop leaves is limited. In an early work, some researchers studied the growth of trees on a rainy scene[8]. Biroun et al.[9] believed that the impact of droplets on any inclined surface is very important for antifreeze, self-cleaning and anti-infection applications. Mao et al.[10] considered the phenomenon of droplet rebound but not the impact of droplet shatter and leaf hair properties on a rebound. Research on droplet shatter is generally based on empirical models, with less visualization[11].

It has become a new method in agricultural research to combine virtual models and physical laws in the virtual scene. The computer simulation method is used to reproduce spray fog in the virtual scene. Physical rules are used to simulate the interaction process between the droplet and the blade, which can effectively and quickly calculate the deposition of fog droplets on the rice leaves. Therefore, combined with the visual characteristics of the virtual plant model, the behavior simulation and deposition calculation methods of spray droplets in the rice canopy are proposed to reveal the physical process of spray droplets in the canopy and the deposition state on the rice leaves. This study provides a new way to investigate the interaction

between droplets and leaves, supporting the calculation of the deposition amount of plant canopy interacting with a sea of droplets, and possibilities for real-time rendering of large-scale plant scene and fog scene interaction.

2 Establishment of virtual fog scene

A three-dimensional simulation model of droplet ejection was established to produce different spray pressure, droplet diameter, jet velocity, jet direction, and spray height, and then simulate different spray scenarios. The velocity of the droplet ejecting from the nozzle, falling to the blade surface, and colliding with it is one of the crucial factors to determine the behavior of the droplet after a collision. The falling velocity of the droplet is related to its density, mass, and diameter, as well as the density of the surrounding air, the flow velocity of the air, and its viscosity coefficient. Therefore, considering these factors comprehensively, a droplet falling velocity solution model based on Newton's second law and hydrodynamic equations is established in research. Then, the velocity of a droplet falling to the surface of the blade under different spray conditions is calculated by using the model.

In this study, a common conical fog scene was simulated to analyze the deposition, retention, spatter, and other behaviors of fog droplets in the virtual fog scene. For an ideal taper fog scene (particle influenced only by gravity, ignoring air resistance, wind, and other external forces), assuming that the particles emerge with a relative velocity V_{init} (m/s) from a nozzle and the direction is gravity, the nozzle motion velocity is V_x (m/s), and the direction of the nozzle motion is the positive direction of the X-axis of the local cartesian coordinate system, the Z-axis, in contrast to the gravity direction. A tangential centrifugal vortex nozzle is selected as the type of nozzle, which can generate conical spray field. According to the kinetic energy is conserved, when the altitude difference between the droplet and the nozzle is h, the velocity of the droplet can meet the requirements:

$$\frac{1}{2}mv_h^2 = mgh + \frac{1}{2}mv_{init}^2 + \frac{1}{2}mv_x^2 \tag{1}$$

where, m is droplet mass, kg; v_h (m/s) is droplet velocity at altitude h (m), and its magnitude is calculated by Equation (2):

$$\left|\overrightarrow{v_h}\right| = \sqrt{2gh + v_{init}^2 + v_x^2} \tag{2}$$

To facilitate the calculation, that the droplets on the cross-section of any height layer in the conical fog scene are evenly distributed, then the deposition amount of a triangular patch on the blade of height layer h in the fog scene is related to the movement velocity of the fog scene, the initial velocity of the droplets, the height difference, the spray amount per unit time, the direction angle of the nozzle and the horizontal mapping area of the patch, as shown in Figure 1. The calculation of the ratio P between the mapping area (S_{map}) of the triangular surface area at the height layer h and the horizontal area (S_h) of the fog scene at the height layer h is as follows.

$$P = \frac{S_{map}}{S_h} = \frac{S_{map}}{\pi(h\cdot\tan\frac{\theta}{2})^2} \tag{3}$$

where, θ is the spray angle of the conical nozzle in a fog scene as shown in Figure 1, (°). S_{map} can be obtained from Equation (4), m².

$$S_{map} = \frac{1}{2}\cdot\begin{vmatrix} x_1 & y_1 & 1 \\ x_2 & y_2 & 1 \\ x_3 & y_3 & 1 \end{vmatrix} = \frac{1}{2}\cdot(x_1y_2 + x_2y_3 + x_3y_1 - x_1y_3 - x_2y_1 - x_3y_2) \tag{4}$$
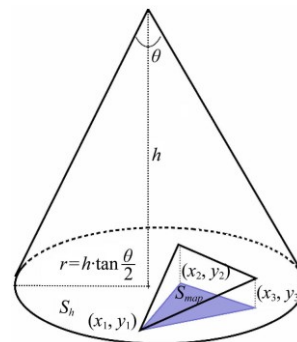
Figure 1　Positional relationship between the triangular patch and the conical spray field

When the droplets fall evenly in the fog scene, the average number of intercepted droplets Sum_i on the ith surface is approximately the product of the spray amount N (unit: granule/s) per unit time, the ratio P of the mapping area of the patch at the height to the horizontal area of the fog scene, and the exposure time interval of the triangular patch in the fog scene, as shown in Equation (5).

$$Sum_i = N \cdot P_i \cdot \Delta t \tag{5}$$

Then, the deposition amount of fog droplets on a leaf Sum_{leaf} is the Sum of the deposition amount of all triangular surfaces:

$$Sum_{leaf} = \sum_{i=0}^{n} Sum_i \tag{6}$$

Suppose Δt is the approximate time of the fog scene passing through the triangular patch. Because the patch size is very small relative to the fog scene, and the process of entering and leaving the fog scene is approximately opposite, the average time of entering and leaving the fog scene is taken as the maximum of the x coordinate difference of the three vertices of the triangular patch, and its calculation Equation (7) is as follows:

$$\Delta t = \frac{\text{Max}\{|x_1 - x_2|, |x_1 - x_3|, |x_2 - x_3|\} + 2h\cdot\tan\frac{\theta}{2}}{V_X} \tag{7}$$

where, V_X is the moving speed of the fog scene, and X_1, X_2, and X_3 are the X-axis coordinates of the triangular surface, respectively.

Traditional rendering technology often has difficulty with realistic simulation of fuzzy phenomena, such as fire, fireworks, water flow, and other scenes. In 3D computer graphics, a common method is to use a particle system to simulate more realistic fuzzy scenes. In this study, the particle system is used to simulate the spray scene and implemented in Unity3D. It can be observed that the movement of larger particles in the fog scene is closer to a vertical falling, and for small particles, it shows diffusion, which is consistent with the spray effect of a mist sprayer in agricultural production. To achieve a more realistic simulation effect of the fog scene, this study adopts the method of superposition of two-particle systems to simulate the hazy fog scene, that is, the fog scene is divided into a high-speed particle system composed of high-speed and large-particle droplets and a slow speed and small particle foggy particle system. To save calculation costs, the particle system in this study does not take a single droplet as a particle, but a collection of ten droplets as a particle. When simulating an ideal cone-shaped fog scene, this study adopts the billboard technology to make all the pixels orthogonal to the angle of view, so only the pixels in the cone-shaped section of the fog scene need to be rendered, instead of the whole fog scene. In the case of improving operation efficiency, the reality of the fog scene can be guaranteed. The specific algorithm is as follows:

Step 1: Set the initial parameters of fog scene

The initial parameters of the fog scene shown in Figure 2 are composed of the following parameters: three-dimensional coordinates of the nozzle (x, y, z) and spray angle of the fog scene θ_a, the spray angle of the mist particle system is set to θ_a, the initial velocity of the element is V_a, the spray angle of the high-speed particle system is set to θ_b, the initial velocity of its primitive motion to V_b, the maximum lifetime of the primitive motion to T_{max}, the maximum height of the fog scene to h_{max}, and the maximum diameter of the fog scene is r_{max}. The initial velocity of the element is the initial velocity of the spray droplet in the spray field, which is in the random direction at the spray angle of the particle system. Two particle systems select different textures to generate materials.
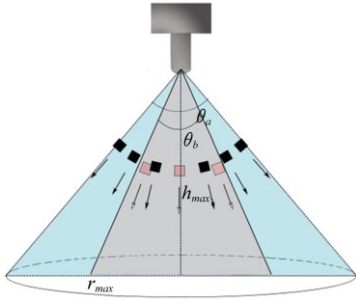
Figure 2   Schematic diagram of fog scene

Step 2: Element update

For the ideal conical fog scene with N spray per unit time (particle/s), if the number of particles contained in the primitives is M, the output time of unit time graphic element Q is N/M up.

Step 3: Element death

If the existence time of the element is greater than T_{max} or its moving height is greater than h_{max}, the element will be destroyed and enter step 5; Otherwise, enter step 4.

Step 4: Element movement

Each time step updates the position of all the elements that have not died out. For the elements whose life cycle is in the ith time step, the position P_i and velocity v_i are

$$P_i = \begin{cases} 0, & (i = 0) \\ P_{i-1} + v_i t, & (i > 0) \end{cases} \quad (8)$$

$$v_i = \begin{cases} v_{init}, & (i = 0) \\ v_{i-1} + g_{i-1} t, & (i > 0) \end{cases} \quad (9)$$

Step 5: Rendering

Render the existing element and return to step 2.

Figure 3a is the simulation result of a mist particle system, taking θ_a=30°. Figure 3b is the simulation result of the high-speed particle system, taking θ_b=25°. The mist particle system is characterized by smaller particles in the fog scene (Figure 3a), which is hazy visually, while the droplet particles in the high-speed particle system are more clearly visible (Figure 3b), Figure 3c is the simulation result of the fog scene generated by the combination of the two, which is more realistic and shows the mist field and the high-speed droplet field at the same time. Figure 3d is the visualization effect of the moving fog scene. Because the droplet velocity in the high-speed field is greater than that in the mist field, according to Newton's law of mechanics, the parabolic trajectories of the two droplets are different, and the high-speed particles and mist particles are staggered. Figure 4 shows the performance of the fog scene in the rice field scene. The real-time FPS is more than 60 frames, which meets the requirements of real-time rendering.

| a. Mist fog scene | b. High-speed fog scene | c. Fog scene superposition | d. Sports fog scene |
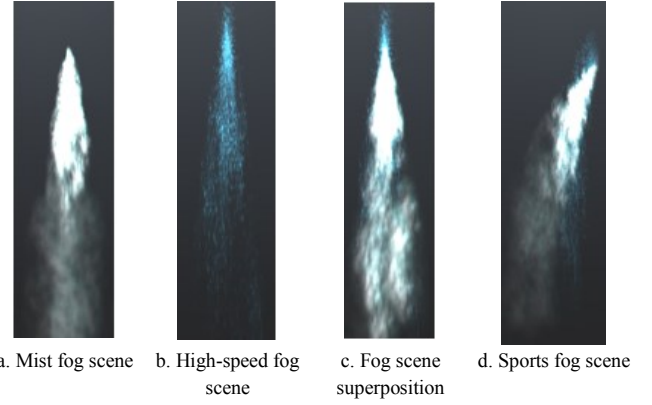
Figure 3   Visualization of fog scene

Figure 4   Motion of fog scene in rice scene

3   Simulation of droplet deposition on blades

Leaf is the main target organ of pesticide spray. Studying and predicting the behavior of a droplet after collision with the blade and predicting the behavior of droplet after collision will help to study the interaction between droplet and plant canopy, and it can be used as a reference for pesticide use. Li et al.[12] also points out that droplet deposition is an important factor in the interaction between droplet and blade. Therefore, the behavior analysis and prediction of droplet impacting on solid surfaces have always been an important direction in fluid research. The behavior of droplet after collision with blade mainly includes droplet rebound, droplet breakage, blade deformation, and so on, which will affect the amount of droplet deposition on the blade surface.

3.1   Effect of droplet rebound on deposition

3.1.1   Judgment of rebound

Mao et al.[10] used a high-speed camera to capture the rebound images of droplets at different temperatures, viscosities, static contact angles, and droplet sizes. By analyzing the images and combining them with the energy analysis in the process of droplet movement, a model based on Reynolds number, Weber number, and static contact angle was proposed to predict the rebound trend of droplets, and an empirical equation was proposed.

$$\left[\frac{1}{4} \left(1 - \cos\theta_s \right) + 0.2 \frac{We^{0.83}}{Re^{0.83}} \right] \left(\frac{d_m}{D} \right)^3 - \left(\frac{We}{12} + 1 \right) \left(\frac{d_m}{D} \right) + \frac{2}{3} = 0 \quad (10)$$

where, d_m/D is the ratio between the maximum expanded diameter d_m and the initial droplet diameter D, and θ_s is the static contact angle. We and Re are two dimensionless quantities in fluid mechanics, which are called Weber number and Reynolds number respectively.

The residual energy E_{ERE} of the droplet is calculated in the regression phase to judge whether the droplet rebounds or stays[10]. When the residual energy is greater than zero, the droplet is considered will rebound, otherwise, the droplet will stay on the blade surface. The equation for calculating the residual energy of droplets is as follows.

$$E_{ERE} = \frac{1}{4} \left(\frac{d_m}{D} \right)^2 \left(1 - \cos\theta_s \right) - 0.12 \left(\frac{d_m}{D} \right)^{2.3} \left(1 - \cos\theta_s \right)^{0.63} \quad (11)$$

3.1.2   Update the velocity of the rebound droplet

When the droplet collides with the blade, part of its potential

energy is converted into the potential energy of the blade, which will deform the blade[13]. At the same time, due to the decrease in the kinetic energy of the droplet, the velocity of the rebound droplet will decrease. The velocity of the rebound droplet is updated as:

$$\left|\overrightarrow{r_{exit}}\right| - \sqrt{\frac{2E_{ERE}}{\pi\rho D^3}} \qquad (12)$$

where, $\left|\overrightarrow{r_{exit}}\right|$ is the velocity of droplets. When predicting the rebound direction of droplets, the probability distribution function was used to simulate the droplet rebound. Moreover, Abbott et al.[14] considered that the rebound direction of raindrops after collision with leaves is related to the roughness of leaves, and its distribution meets certain statistical rules. The change of the rebound angle of droplets satisfies the Gaussian distribution, that is, the rebound angle offset value $x \sim N(\mu, \sigma^2)$.

3.1.3 The influence of fuzz on the rebound

Leaf hairs, which are trichomes on the leaf surface, are a feature of rice. Rice can be divided into hairy and hairless varieties. In previous studies[10,16], the method for judging the rebound only considered leaf roughness, but not the impact of hairs. When the hairs on the leaf are dense, the droplet can be easily dragged but difficult to rebound. This study proposes that the hairs produce a drag force F_{drag} (N). F_{drag} is the sum of all hairs in contact with the droplets and is decided by contact area, droplet gravity, and hair density droplet. E_{drag} (J) is the energy that is overcome by F_{drag} and proportional to the hairs' average length l:

$$E_{drag} = \sum F_{drag} l \qquad (13)$$

Therefore, based on the literature[10], the modified residual energy E'_{ERE} is corrected as follows:

$$E'_{ERE} = E_{ERE} - E_{drag} = \frac{1}{4}\left(\frac{d_m}{D}\right)^2 (1 - \cos\theta_s) - 0.12\left(\frac{d_m}{D}\right)^{2.3}(1 - \cos\theta_s)^{0.63} - E_{drag} \qquad (14)$$

Besides, the rebound velocity is:

$$\left|\overrightarrow{r_{exit}}\right| - \sqrt{\frac{2(E_{ERE} - E_{drag})}{\pi\rho D^3}} \qquad (15)$$

3.2 Effect of droplet shatter on deposition

In the study of droplet depositions in spray scenes, it is generally believed that after the droplets collide with leaves, they will only rebound off or stay on the canopy. After flowing, gathering, and splitting, some of the droplets that stay will eventually deposit on the leaf surface. However, in the study of fluid mechanics, droplet behavior not only rebounds but also shatters[15]. Researchers used high-velocity cameras to observe the impact of droplets and found that the droplets will spread like a disc on the surface after colliding. Besides, if the inertia of a droplet overcame the surface tension maintaining its shape, a shatter will occur.

Different from the droplets that completely rebounded off, the shattered droplets' volume and kinetic energy are smaller and easier to retain on the leaf surface. Moreover, the retained droplets that did not shatter will lose their kinetic energy. A droplet shatter modeling method was established that is suitable for rice leaves.

3.2.1 Judgment of shatter

During droplet shatter, the droplets will produce two types of sub-droplets: $Drop_{shatt}$ indicates the shattered droplets that overcame the capillary action, and $Drop_{retain}$ is the retained shattered droplets on the surface. For judging whether droplet shatter occurs or not, Mundo et al.[15] proposed the following decision method:

$$K > K_{crit} \qquad (16)$$

where, K is the dimensionless eigenvalue of the droplet, determined by the Weber number and Reynolds number[17]. K_{crit} is a characteristic threshold, which is related to the surface characteristics of the impacted blade. When $K > K_{crit}$, a shatter will occur.

On the horizontal surface, the characteristic threshold K_{crit} is positively correlated with the droplet contact angle[18]. Extending it to inclined surfaces, the value of K_{crit} is determined by the sum of the advancing contact angle (ACA) and receding contact angle (RCA) of the droplet on the inclined blade. ACA and RCA are measured using a contact angle meter.

3.2.2 Simulation of droplet shatter

When droplets shatter, several little droplets $Drop_{shatt}$ will be generated, and a retained droplet $Drop_{retain}$ will stay on the blades. The motion simulation of the shattered droplets needs to be conducted. The volume of the retained droplets and the total volume of the shattered droplets will be calculated separately, including the number, diameter, and velocity of shattered droplets. The details are as follows:

(1) The total volume of the shattered droplets $Vol_{shatter}$ and the volume of the retained droplet Vol_{retain} are:

$$Vol_{shatter} = (1 - p)\pi D_{init}^3 / 6 \qquad (17)$$

$$Vol_{retain} = p\pi D_{init}^3 / 6 \qquad (18)$$

where, D_{init} is the initial diameter of the droplet, mm; p is the ratio of the droplet shatter, which is related to the spreading behavior of the droplets[16], and its value is between 0 and 1.

(2) The number of shattered droplets $N_{shatter}$:

At least one shatter droplet will be generated and the maximum is indicated as Max. $N_{shatter}$ can be expressed as:

$$N_{shatter} = \text{random}(1, Max) \qquad (19)$$

(3) The diameter of the single shattered droplet $D_{shatter}$ (mm) can be calculated using $Vol_{shatter}$ and $N_{shatter}$:

$$D_{shatter} = \sqrt[3]{\frac{6Vol_{shatter}}{\pi N_{shatter}}} \qquad (20)$$

(4) The velocity directions of the shattered droplets:

The motion direction of the shattered droplets can be calculated in the local coordinate system of the collision surface, as shown in Figure 5, where S is the collision surface, and α and β are the direction and altitude angles, respectively. The small droplets after shattering are conical and uniformly distributed. Therefore, α of the ith shattered droplet is

$$\alpha = 360° + i \times 360° / N \qquad (21)$$

The altitude angle β satisfies the normal distribution, $\beta \sim X(u, \delta)$, which is between 0° and 90°.
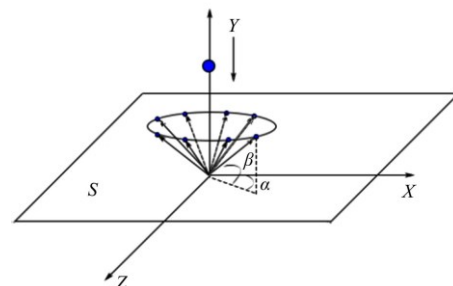
Figure 5   Schematic diagram of droplet shatter

(5) The velocity of shatter droplets $V_{shatter}$:

The droplet rebound is a special case of shatter. When the droplet rebounds, it is considered as shattering, where $p=0$ and

$N_{shatter}=1$. Similar to the velocity equation of the droplet rebound, the velocity of the droplet shatter satisfies the following:

$$\left|\overrightarrow{r_{shatter}}\right| = \sqrt{\frac{12E_{shatter}}{\pi N_{shatter}\rho D_{shatter}^3}} \tag{22}$$

$$E_{shatter} = (1-p)E_{impact} \tag{23}$$

where, $E_{shatter}$ is the kinetic energy of the shattered droplet, and E_{impact} is the kinetic energy of the droplet during the collision, which is calculated according to the conservation of kinetic energy.

3.3   Effect of rice leaf deformation on deposition

Rice leaves will deform under the action of the fog scene, which will affect the real deposition of fog droplets. This section combines the previous research on leaf deformation under wind field[19] and extends it to the effect of fog scene on rice leaf deformation in this study.

In the simulation of blade deformation, the external force on the blade is time-varying. When the blade vibrates, it is usually necessary to solve a complex differential equation. In this study, the influence of vibration on the deposition is not considered when calculating the deposition amount under the condition of blade deformation, and the following assumptions are made: 1) the deformation of the blade quickly reaches the equilibrium state after the whole blade enters the fog scene; 2) the influence of blade vibration on the deposition amount is ignored, and the deposition amount under the blade equilibrium state is taken as the criterion when calculating the deposition amount; 3) it is considered that the blade equilibrium state reaches the maximum deposition amount under the blade equilibrium state.

In the simulation of rice leaf deformation, several control points are marked on the rice leaf, and the bottom of the leaf is taken as the root node. The root node remains motionless in the fog scene, and the deformation between two adjacent control points is not affected by the force between other control points. The movement of the whole leaf is simulated by calculating the displacement of the control points. As shown in Figure 6: P_0 is the root node. Under the action of the fog scene, the rotation angle of some blades between line segments P_0P_1 is determined by all triangular patches between line segments P_0P_1. When line segment P_0P_1 reaches the equilibrium state, the combined external force F_{01} on the blade is 0, and the combined external force is the sum of the combined external forces on all triangular patches on the blade.

$$P_{01} + W_{f01} + R_{01} = 0 \tag{24}$$
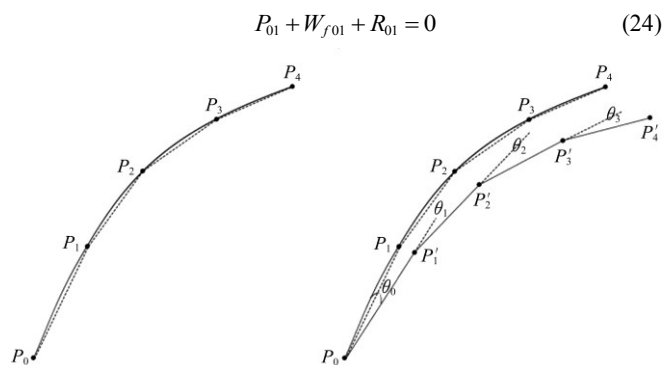
Figure 6   Side view of rice deformation

The pressure P_{01} is equal to the sum of the gravity components of the deposition droplets along the radial direction of the blade when the maximum deposition amount is reached on n patches:

$$P_{01} = \sum_{i=0}^{n} P_i \tag{25}$$

The continuous pressure W_{f01} is the sum of N patch pressures:

$$W_{f01} = \sum_{i=0}^{m} W_{fi} = \sum_{i=0}^{m} S_{mapi}\sigma'\left|\overrightarrow{r_h}\right|_i \tag{26}$$

$$W_f = \sigma'\psi S_{mapi}\left|\overrightarrow{r_h}\right| \tag{27}$$

where, W_{fi} is the force exerted on a single surface by the fog field, S_{mapi} is the horizontal mapping area of the surface, and σ' is the drag coefficient of the fog field and the droplet velocity. ψ represents the density of droplets, and its calculation equation is as follows.

$$\psi = \frac{N}{S_h} = \frac{N}{\pi\left(\dfrac{h}{\tan\dfrac{\theta}{2}}\right)^2} \tag{28}$$

where, N is the number of droplets per unit time, grain/s, and S_h is the cross-sectional area of the fog field when the height layer is h.

The recovery force R_{01} between P_0 and P_1 is calculated according to the following equations[20].

$$R_{01} = K_{01}\Delta\theta_{01}l_{01} \tag{29}$$

$$\Delta\theta_{01} = \frac{P_{01} + W_{f01}}{-K_{01}l_{01}} \tag{30}$$

where, $\Delta\theta_{01}$ is the deflection angle of P_0, and so on, the deflection angle of node P_i can be obtained by analogy. In actual deflection, the deflection angle of P_i is the sum of the calculated angle and the deflection angle of its predecessor nodes.

3.4   Fitting method of maximum deposition on Rice Leaves

The deposition amount refers to the deposition droplets staying at the target position, which is generally expressed by droplet volume. This study refers to the number of droplets staying on the surface of rice leaves. The maximum deposition on a triangular patch refers to the maximum number of droplets that can be attached to the triangular patch. Its value is related to the geometric shape of the triangular patch (area and inclination), as well as the surface material characteristics, droplet size, and droplet characteristics.

Table 1   Maximum number and average diameter of droplets deposited on rice leaves

Serial number	1	2	3	4	5
Number of droplets	972	995	1200	1381	1440
Average diameter/mm	0.460	0.556	0.627	0.666	0.301

Sedimentation tests were conducted on the potted tiller rice at the China Rice Research Institute. This study screened the number of droplets and droplet radius of rice leaves that were adequately sprayed and used the number of droplets as the basis of maximum deposition. Some data on droplets deposited on some rice leaves were obtained.

Song et al.[19] considered that there is an attractive force H between two droplets. When the attractive force is greater than the friction force, the two droplets will move towards each other, merge into a large droplet and flow:

$$H(d) = -\log\left(\frac{d}{r_1 + r_2}\right) \tag{31}$$

where, d is the center distance of droplets, and r_1 and r_2 are the radii of droplets respectively.

It is obtained that in the horizontal plane, the radius R and the contact angle θ of the droplet ball, and the radius r of the falling droplet satisfy the following conditions:

$$r = \sqrt[3]{\frac{4}{2 - 3\cos\theta + \cos\theta^3}}R \tag{32}$$

When the droplets are densely distributed on the triangular patch, R is the average radius of the droplets on the blade. When the droplet spacing $d=kr$ (k is the user preset coefficient, $k>2$), the blade reaches the maximum deposition, in this case.

$$S_{leaf} = N_{max}(d+r)^2 = (1+k)^2 N_{max}r^2 \qquad (33)$$

Among them, S_{leaf} is the horizontal projection area of rice, and N_{max} is the largest deposition amount. When the number of droplets deposited is larger than N_{max}, the droplets cannot be intercepted completely. Besides, the value of d is related to the type of leaves. Due to the small size of the falling droplets, after the droplets collide with the blades, the droplets that are closer to each other will merge into a larger droplet. When the droplet volume accumulates to a certain extent, the droplet will flow on the inclined blade when the friction force is less than the gravity component of the droplet. To simplify the calculation, the influence of droplet flow on deposition is not considered, but there is a threshold value N_{max} of deposition quantity on rice leaves. When the number of deposition droplets on rice leaves reaches N_{max}, the deposition droplets will roll and leave the leaves. In the process of rice spraying, droplet deposition increases with height, and the larger the dip angle, the larger the contact area with the droplet field and the greater the deposition capacity[20]. In this study, it is assumed that the maximum deposition number N_{tri} on any triangular patch on the virtual rice model is proportional to the projected area S'_{tri}.

$$N_{tri} = \frac{S'_{tri}}{S_{leaf}} N_{max} \qquad (34)$$

The volume sum of all the droplets deposited on the triangle can be calculated, which is recorded as Vol.

$$Vol = \frac{4\pi N_{tri}}{3} R^3 \qquad (35)$$

3.5   Algorithm design of droplet deposition on the leaf surface

Based on the above research ideas, a method for counting the number of droplets deposited on rice leaves based on a virtual fog scene is proposed in this study. The main implementation steps are as follows:

Step 1: initialize the fog scene attribute and build a conical fog scene.

Step 2: import the parameterized rice leaves and calculate the maximum deposition on each triangular patch.

Step 3: to avoid a lot of unnecessary collision detection, preprocess the fog scene and rice leaves. For all triangular patches of leaves, according to their position relationship with the conical fog scene, calculate their entry time t_1 and departure time t_2 in the fog scene, and only carry out collision detection between t_1 and t_2.

Step 4: according to the movement track of the droplet, collision detection is carried out between the droplet track and the mesh bounding box of the blade. If the droplet track passes through the mesh bounding box of the blade, go to step 5, otherwise, go to step 8.

Step 5: according to the residual energy to judge the rebound of droplets: if there is a rebound, simulate its rebound trajectory, go to step 8, and the droplet is not included in the deposition; if there is no rebound, go to step 6.

Step 6: if the droplets are broken, the remaining droplets are included in the deposition. According to the trajectory of the broken droplets, whether the broken droplets can stay on the leaf is checked. If the broken droplets can stay on the blades, the broken droplets are included in the deposition.

Step 7: update rice leaf structure based on current droplet deposition.

Step 8: update the position of the droplet in real time. When the height of the droplet is lower than the ground level, the particle will die out.

Step 9: count the current droplet deposition amount on the triangular patch at each time step. When the amount of droplet deposition is greater than or equal to the maximum deposition amount, the triangular patch cannot continue to receive droplets.

4   Results and analysis

Before the experiment, the parameters in the fog scene were set, mainly including the construction of the fog scene model, nozzle parameter setting, and rice leaves. The fog scene model of the deposition statistics method in this study adopts the construction method of the conical fog scene described in Section one and assumes that the fog scene is not affected by wind speed and other factors. In this study, the main variable factors are the range of initial velocity of droplets, droplet size, spray angle, and spray amount per unit of time. The initial velocity range of droplets is set between 0.5-2.5 m/s, the droplet size is between 100-500 μm[22], the nozzle angle is 30°-70° and the spray amount per unit time can be calculated according to the nozzle flow and droplet size; 3000 cm³/s, 4000 cm³/s, 5000 cm³/s, and 6000 cm³/s are used respectively.

4.1   Simulation of rebound and shatter

In the visualization of droplet rebound, the quadratic Bézier curve was utilized to simulate the rice leaves and the particle system was employed to simulate the droplet motion. The maximum number of droplets in the scene is 3000, and FPS is above 40. This study uses different initial velocities to simulate the droplets. Figures 7a-7d show the results of the initial velocity of hairless leaves: 0.5-1.0 m/s, 1.0-1.5 m/s 1.5-2.0 m/s, and 2.0-2.5 m/s, respectively. The results show that with the increasing droplet velocity, the disturbance range of rebound directions on the horizontal blades and the rebound velocity is increased; With the increase of droplet velocity range, more droplets rebound off the leaves, which weakens the deposition effect of the spray. Therefore, choosing the appropriate sprayer aperture and spraying velocity is important to improve the effectiveness of the spray and reduce waste. The results of this study are similar to those in a previous study[5].

a. Initial velocity 0.5-1.0 m/s   b. Initial velocity 1.0-1.5 m/s

c. Initial velocity 1.5-2.0 m/s   d. Initial velocity 2.0-2.5 m/s
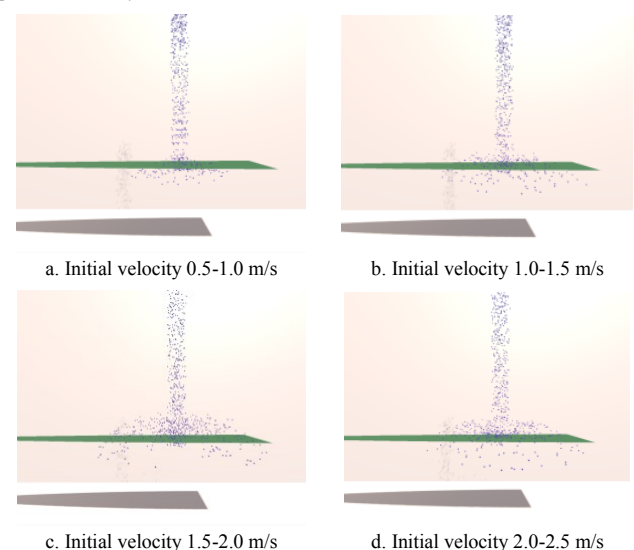
Figure 7   Droplets rebound on the horizontal leaves at different velocities

When droplets collide with inclined blades, the rebound direction is symmetrical with the incident angle if the disturbance caused by leaf roughness is not considered[16].   In this study, the Gauss distribution was used to increase the disturbance of the rebound so that the exit angle was more realistic.   Figure 8 shows the visualization results of rebound direction with and without disturbance on the inclined leaf, leaf angle of 30°, and droplet initial velocity of 1.0-1.5 m/s.   Figure 9 shows the rebound visualization results on hairy and hairless leaves, with an initial velocity of 1.0-1.5 m/s and κ of 1.5.   As shown in Figure 9, the droplets on the hairless leaves have higher rebound velocity but lower horizontal spread than those on hairy leaves.

a. Rebound without disturbance   b. Rebound with leaf roughness
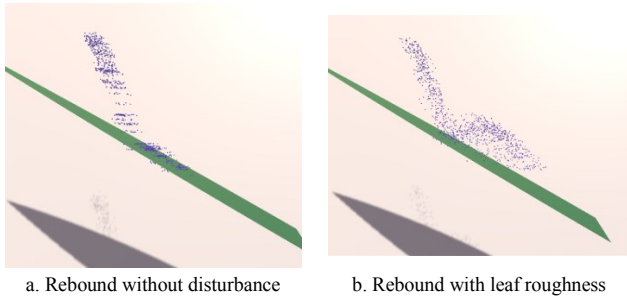
Figure 8   A rebound of droplets on inclined blades

a. Rebound on a hairless leaf   b. Rebound on hairy leaf
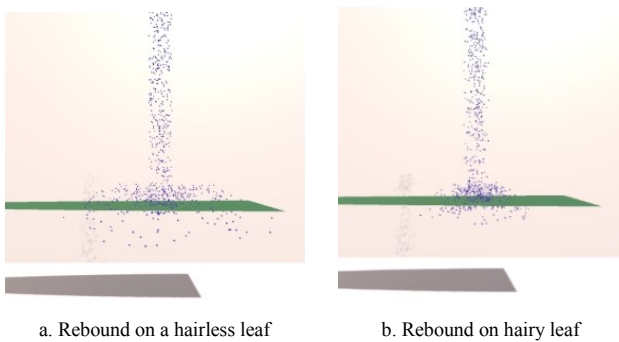
Figure 9   Effect of plant hairs on the rebound

As kinetic energy for droplet rebound is greater than that for droplet shatter, in the visualization process, the rebound is first determined.   If the droplet does not rebound, then it is considered broken.   Figure 10 shows the droplet rebound and shatter occurring together, where the shattered droplets are red and the rebound droplets are blue.   The initial velocity is 1.5-2.5 m/s.
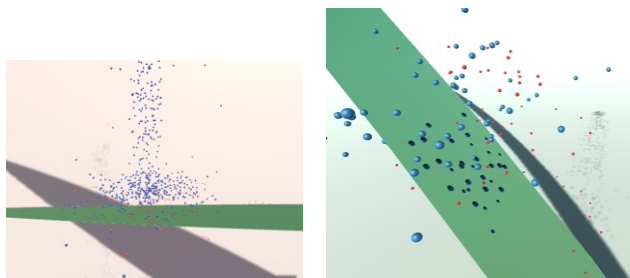
Figure 10   Rebound and shatter droplets

4.2   Effect of nozzle angle on droplet deposition on the blade

First, the influence of nozzle angle on droplet deposition was virtually measured.   The nozzle angle was 30°, 40°, 50°, 60°, and 70°, respectively.   The number of droplets per second was 6000, the initial velocity of spray was 1.0 m/s, and the height of the nozzle was 1.0 m, and it is assumed that the droplet diameter produced by the nozzle is 200 μm.   Here, the deposition efficiency is defined as the number of droplets deposited on a unit leaf area per second.   The test results are shown in Figure 10.   The

experimental results show that (1) at the same injection speed, the greater the angle of the nozzle, the lower the deposition efficiency of droplets on the blade; (2) The time to reach the maximum deposition volume increases with the increase of the spray angle; (3) The larger the spray angle, the higher the upper limit of the maximum deposition volume on the blade, that is, the blade can retain more liquid medicine.   The results show that: (1) and (2) are caused by the smaller the spray angle, the smaller the coverage of the fog scene, and the increase in the deposition of fog droplets at the same time.   (3) The reason is that the small spray angle cannot completely cover the fog scene, resulting in no droplet deposition in some locations.   Therefore, it is particularly important to select a suitable nozzle angle in rice spray.   When the spraying crops are more efficient, a small angle nozzle can be selected.   When the spraying crops are adequately sprayed, a large angle nozzle can be selected.   This conclusion is similar to the result of the research on the spray direction angle and deposition amount in agriculture[23].

The influence of the nozzle height on the deposition rate was measured.   The nozzle height was 0.5-1.1 m, the droplet ejection amount per second N was 6000, the initial velocity of spray was 1.0 m/s, the droplet diameter was 200 μm, and the nozzle angle was fixed at 60°.   The result is shown in Figure 11.   It can be seen that: (4) with the increase of nozzle height, the deposition efficiency of blade decreases; (5) when the height of fog scene is 0.5-0.9 m, the maximum deposition increases with the height of fog scene, and when the height of fog scene is 0.9-1.1 m, the maximum deposition is unchanged.   In this study, the analysis shows that: the reason for the formation of the fog scene is similar to that of the first two, which is caused by the coverage of the fog scene; the reason for the formation of the fog scene is that when the height of the fog scene is 0.5-0.9 m, the fog scene does not completely cover the whole leaves, and after 0.9 m, the fog scene can completely cover the leaves.   Therefore, in the actual field operation, the selection of suitable height nozzles has a significant effect on improving deposition efficiency.   According to literature [23], the spray device that has the best distance from the crop is similar to the results in this study.

It is worthy of note that the number of droplets in Figures 11 and 12 is the number of droplets per unit area of the blade. Moreover, in Figure 12, the nozzle was at different heights, while the interaction points on the X-axis were very close.   Here, the settling times of droplets at different heights are not considered, because there is little difference in settlement time at different heights.
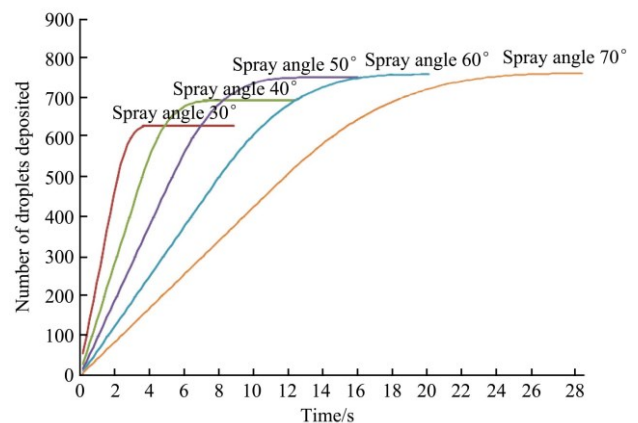
Figure 11   Comparison of the number of droplets deposited on blades at different spray angles
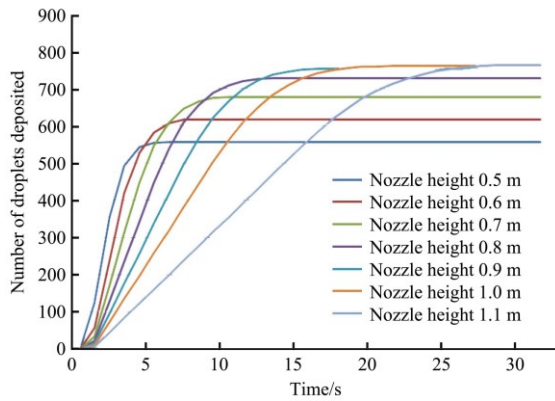
Figure 12   Comparison of the number of droplets deposited on the blade under different nozzle heights

4.3   Discussions

To improve the realism of the simulation of interactions between droplets and leaves, this study analyzes the rebound and shatter of droplets by combining relevant methods of fluid mechanics.   Compared with previous works, this study combines the droplet rebound with the actual situation of rice; for example, the transformation of rice leaf under the influence of spray was added to judge droplet rebound.   Moreover, a method to determine the threshold value of the droplet shatter was proposed.   For rendering, Unity3D and the graphics capabilities of the GPU were used to simulate rebound and shatter.

In this study, a two-layer particle system was used to simulate the fog scene, and the fog scene is divided into high-speed field and mist field.   However, the defined conditions of high-speed field and mist field lack in-depth discussion.   Therefore, it simulated the influence of the motion of the fog scene on the appearance of the particle system but ignored the influence of the wind force on the shape of the fog scene.   In addition, due to the lack of tools to measure the drag force of fuzz on droplets, this study simply sets a parameter as the drag coefficient, which is not accurate.   In the aspect of droplet breakage judgment, this study uses the relationship between the measured droplet inclination angle and the front and rear contact angle as the judgment basis, but due to the limitation of measurement accuracy, there are inevitably errors. For the calculation of droplet deposition, because the droplet size is small, the droplet will flow only when the droplets converge into several large droplets and reach the maximum deposition.   In fact, due to the influence of the kinetic energy of the droplet itself, droplets on an inclined blade are more likely to flow.   In the future, we can continue to go deep into the physics law of droplet flow, to make it more realistic.

5   Conclusions

In this work, a method to simulate and visualize spraying droplets' behavior and deposition within virtual rice canopy was proposed.   This method combines the established fog scene model and rebound fragmentation model, and considers the influence of the deformation of the blade caused by the fog scene on the deposition.   On this basis, a method to determine the maximum deposition on the blade is proposed.   The visual stimulation of the interaction between fog and leaves of a rice plant is realized on the Unity3D platform.   The experiment shows that the simulation platform can be used to study the mechanism of spray deposition in the canopy of the rice plant.   In the future, the proposed method will be used for other crops (such as cotton, and wheat) and also be utilized to simulate the influence of wind on the high-speed field

and mist field respectively.   Moreover, the influence of the fluff characteristics on the deposition will be considered, to make the virtual deposition statistical model more accurate.

[References]

[1]   Xu D J, Gu Z Y, Xu G C, Xu X L.   Influence of sprayer and application rate on pesticide deposit character on rice canopy.   Scientia Agricultura Sinica, 2013; 46(20): 4284–4292.

[2]   He X K.   Improving severe draggling actuality of plant protection machinery and its application techniques.   Transactions of the CSAE, 2004; 20(1): 13–15. (in Chinese)

[3]   Song S R, Wang W X, Hong T S, Wang P, Luo X W.   Testing research on effects of top layer rice fog drop interception on pesticide spraying distribution in rice fields.   Transactions of the CSAE, 2003; 19(6): 114–117. (in Chinese)

[4]   Huang S W, Liu L M, Wang L, Liu E Y, Fang Z L, Xiao F D.   Effects of application volume and approaches of pesticide on controlling major pests and diseases on different plant type rice at late growth stage. Chinese Journal of Rice Science, 2012; 26(2): 211–217. (in Chinese)

[5]   Smith D B, Shaw D R, Boyette M, Askew S D, Morris W H.   Droplet size and leaf morphology effects on pesticide spray deposition. Transactions of the ASAE, 2000; 43(2): 255–259.

[6]   Yang X W, Dai M L, Song J L, Zhao J K, He X K.   Effect of droplet size, leaf characteristics and angle on pesticide deposition.   Transactions of the CSAE, 2012; 28(3): 70–73. (in Chinese)

[7]   Yang M G, Wu E H.   Approach for physically-based animation of tree branches impacting by raindrops.   Journal of Software, 2011; 22(8): 1934–1947. (in Chinese)

[8]   Rutter A J, Morton A J.   A predictive model of rainfall interception in forests.   III.   Sensitivity of the model to stand parameters and meteorological variables.   Journal of Applied Ecology, 1977; 14(2): 567–588.

[9]   Biroun M H, Rahmati M, Tao R, Torun H, Jangi M, Fu Y Q.   Dynamic behavior of droplet impact on inclined surfaces with acoustic waves. Langmuir, 2020; 36(34): 10175–10186

[10]   Mao T, Kuhn D C S, Tran H.   Spread and rebound of liquid droplets upon impact on flat surfaces.   Aiche Journal, 1997; 43(9): 2169–2179.

[11]   Gary J D, Forster W A, Lisa C M, McCue S W, Kempthorne D M, Hanan J.   Spray retention on whole plants: modelling, simulations and experiments.   Crop Protection, 2016; 88: 118–130.

[12]   Li J, Cui H J, Ma Y K, Xun L, Li Z Q, Yang Z, et al.   Orchard spray study: a prediction model of droplet deposition states on leaf surfaces. Agronomy, 2020; 10(5): 747.   doi: 10.3390/agronomy10050747.

[13]   Liu Y Q, Liu X H, Wu E H.   Real-time 3D fluid simulation on GPU with complex obstacles.   Proceedings of Pacific Conference on Computer Graphics and Applications, IEEE, 2004; pp.247–256.

[14]   Abbott J P R, Zhu H P, Ambrose A E.   Impact and adhesion of surfactant-amended water droplets on leaf surfaces related to roughness. Transactions of the ASABE, 2020; 63(6): 1855–1868.

[15]   Mundo C, Sommerfeld M, Tropea C.   Droplet-wall collisions: Experimental studies of the deformation and breakup process. International Journal of Multiphase Flow, 1995; 21(2): 151–173.

[16]   Dorr G J, Hanan J, Woods N, Ricci P, NollerDorr B.   Combining spray drift and plant architecture modeling to minimise environmental and public health risk of pesticide application.   International Congress on Modelling

and Simulation (MODSIM05), 2005; 1(3): 1499–1500.

[17] Yi X Y, Zhu Y J, Yang J M.   Influence mechanism of initial deformation of droplets after excitation waves under similar Weber number conditions. Explosion and Shock Waves, 2018; 38(3): 525–533.

[18] Forster W A, Mercer G N, Schou W C.   Process-driven models for spray droplet shatter, adhesion or bounce.   Proc. Int. Symp. Adj. Agrochem, 2010; pp.277–285.

[19] Song C F, Peng Q S, Ding Z A, Tu X L, Zhang Y B, Chen W, et al.   Sketch-based modeling and animation of floral blossom.   Journal of Software, 2007; 18(Supp): 45−53. (in Chinese)

[20] Yi L, Lee R R, Chu H K, Chang C F.   A simulation on grass swaying with dynamic wind force.   ACM SIGGRAPH Symposium on Interactive 3D Graphics and Games, ACM, 2016; pp.181–181.

[21] Song S R, Wang W X, Hong T S, Wang P, Luo X W.   Experimental study on the influence of spray droplet interception on the top layer of pesticide spray in paddy field.   Acta Agri Engineering, 2004; 19(6): 114–117.

[22] Yan M D, Jia W D, Mao H P, Dong X, Chen L.   Experiment on spray droplet size and velocity distribution of air curve spray rod. Transactions of the CSAM, 2014; 45(11): 104–110. (in Chinese)

[23] Rutter A J, Kershaw K A, Robins P C, Morton A J.   A predictive model of rainfall interception in forests.   Derivation of the model from observations in a plantation of Corsican pine.   Agricultural Meteorology, 1971; 9: 367–384.